Design and Fabrication Considerations, Numerical Modelling, and Testing of a MEMS Microgripper

Marija Cauchi*, Pierluigi Mollicone
Department of Mechanical Engineering
Faculty of Engineering
University of Malta
Msida, Malta
*mcauc03@um.edu.mt, pierluigi.mollicone@um.edu.mt

Bertram Mallia
Department of Metallurgy and Materials Engineering
Faculty of Engineering
University of Malta
Msida, Malta
bertram.mallia@um.edu.mt

Ivan Grech, Barnaby Portelli, Nicholas Sammut
Department of Microelectronics and Nanoelectronics
Faculty of Information and Communication Technology
University of Malta
Msida, Malta
ivan.grech@um.edu.mt, barnaby.portelli@um.edu.mt, nicholas.sammut@um.edu.mt

***Abstract*—Microgrippers play an important role in the manipulation of biological cells and tissues. This paper presents a horizontal electrothermally actuated microgripper that is designed for the handling and deformability characterisation of human red blood cells (RBCs). Pathological alterations in the mechanical properties of RBCs have been associated with a number of specific diseases. This has accentuated the significance of analysing the deformability characteristics of RBCs within the biomedical field. A polysilicon microgripper structure was designed and fabricated according to the dimensional specifications imposed by the commercial PolyMUMPs™ fabrication process. The microgripper design was developed and numerically modelled using finite element analysis where coupled electrothermomechanical simulations were carried out in CoventorWare®. The fabrication method is presented in this paper, together with details of the experimental set-up used for the actuation testing. The tip displacement of the microgripper arm when electrothermally actuated is compared with that obtained by means of numerical simulations. Results show that the microgripper arm deflected as designed when electrothermally actuated, with good agreement obtained between simulation and experimental results. This paper also proposes critical design and fabrication considerations that were implied from the experimental campaign performed in this work and that take into account out-of-plane buckling of the hot arm, fracture of the arms in the vicinity of the anchored probe pads, residual stresses, and device stiction. Such considerations are regarded as an important outcome of this work, and they must be thoroughly investigated to mitigate the malfunction or failure of the microgripper.**

***Index Terms*—microgripper, electrothermal actuation, red blood cells, fabrication, PolyMUMPs™, buckling, fracture, residual stresses, stiction**

I. Introduction

Microgrippers are typical microelectromechanical systems (MEMS) that are widely used in microassembly and micromanipulation fields. They are designed to safely handle and manipulate micro-objects, such as biological cells [1] and micromechanical parts [2]. Electrothermal actuators have several advantages over other types of actuation mechanisms, such as electrostatic, electrothermal, piezoelectric, pneumatic and electromagnetic, in that they can generate a relatively large output force and displacement with a small applied voltage. Their operating principle relies on the differential thermal expansion of well-designed structures induced via Joule heating [3], [4].

Different studies [5]–[7] have shown the important role of MEMS microgrippers in the manipulation and characterisation of cells and tissues for biomedical applications. The microgripper presented here is designed for the handling and deformability characterisation of human red blood cells (RBCs). Different laboratory procedures have been developed to enable RBCs to be reliably tested in air [8]. A single, biconcave, disk-shaped RBC is approximately 8 μm in diameter and around 2 μm in thickness, and its primary function is to carry oxygen from the lungs to the body tissues, as well as carbon dioxide (CO_2), as a waste product, away from the tissues and back to the lungs. The deformability characteristics of healthy RBCs allow them to flow through capillaries with smaller diameters, in the process supplying oxygen to tissues of the body. Pathological factors, including among others malaria, sickle cell anemia, diabetes and hereditary disorders, hinder the capacity of RBCs to undergo cellular deformation, and consequently to deliver oxygen to the biological tissues (Fig. 1). Due to its pathophysiological significance, measurement of the deformability properties of RBCs has been the subject of numerous studies over the years [9], [10].

This paper gives an overview of the design, numerical modelling and experimental testing of a fabricated horizontal electrothermal MEMS microgripper, accompanied by the identification of critical design and fabrication considerations resulting from the experimental campaign performed in this work. It first presents the microgripper design and its

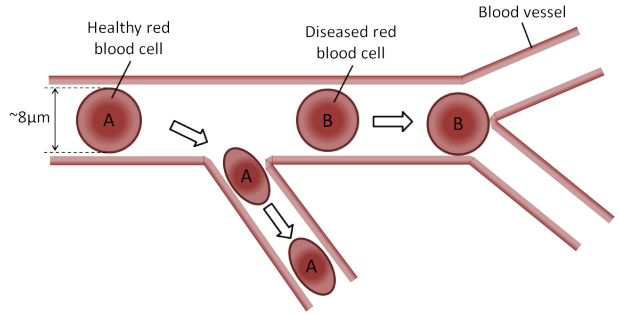

Fig. 1: Schematic illustration of red blood cells (RBCs) within a blood vessel. A healthy RBC (Cell A) can undergo the necessary deformation to freely flow through the smaller blood vessels unlike a diseased RBC (Cell B) whose impaired deformability characteristics inhibit such an ability.

operating principle in Section II, together with a description of the PolyMUMPs™ process used for fabrication of the microgripper in Section III. Section IV highlights the finite element analysis (FEA) model and the implemented modelling techniques. The experimental set-up is given in Section V, followed by an overview of important microgripper design and fabrication considerations in Section VI. The experimental and numerical results for temperature and tip displacement are presented and compared in Section VII. Section VIII summarises the findings and presents the concluding remarks.

II. Microgripper Design and Operating Principle

The microgripper studied in this work is based on a 'hot and cold arm' actuator design as presented in [11], and the electrothermal actuation principle (Fig. 2). A complete microgripper consists of two 'hot and cold arm' actuators that are placed anti-symmetrically next to each other, having extended microgripper arms at their ends to amplify the achieved tip displacement. Electrothermal actuation relies on the asymmetric thermal expansion of the hot and cold arms that is achieved through resistive heating of the suspended polysilicon structure. With the flow of an electric current, the narrower arm experiences greater resistive heating and thermal expansion than the wider arm, resulting in lateral bending of the actuator tip towards the 'cold' arm side. The larger the temperature difference between the hot and cold arms, the higher is the operating efficiency of the horizontal actuator in terms of a larger in-plane displacement achieved for the same applied voltage [3], [4].

III. Fabrication Process

The microgripper was fabricated using the commercial PolyMUMPs™ process [12]. The fabricated microgripper structure consists of one polysilicon structural layer (Poly1) with anchored metal probe pads (Poly1 + Poly2 + Metal) at one end of the actuators (Fig. 3). The microgripper's geometrical dimensions are given in Table I. The mechanical and sacrificial film layer thicknesses are constrained by the

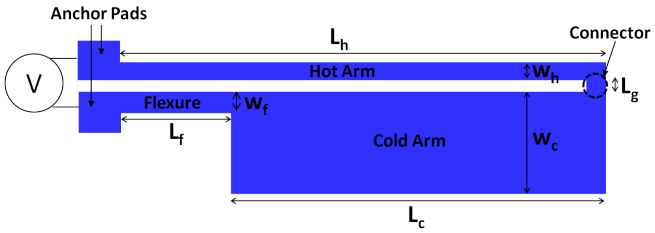

Fig. 2: Schematic diagram of a 'hot and cold arm' electrothermal actuator design with labelled dimensions.

fabrication process, and the layers are photolitographically patterned and etched by means of reactive ion etching to obtain the final wafer pattern. A standard hydrofluoric (HF) solution release designed to fully remove the sacrificial phosphosilicate glass (PSG) layers from the fabricated structure was performed, followed by supercritical CO_2 drying.

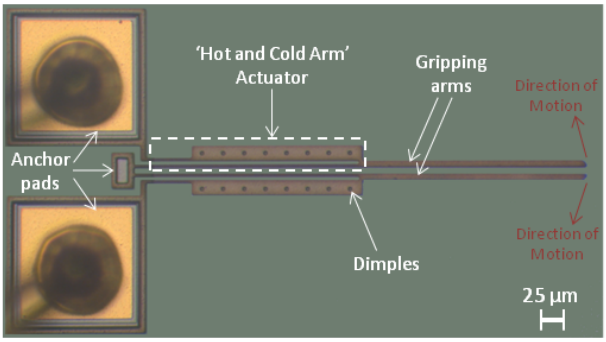

Fig. 3: Optical microscope image of the fabricated polysilicon microgripper structure with a thickness of 2 µm and an air gap of 2 µm beneath it. The black dots seen on the cold arm are dimples included to prevent stiction to the substrate.

TABLE I: Geometrical data of the fabricated microgripper.

Parameter	Value	Unit
Length of hot arm, L_h	200	µm
Length of cold arm, L_c	154	µm
Length of flexure, L_f	46	µm
Length of connector, L_g	3	µm
Length of gripping arm	200	µm
Width of hot arm, w_h	3	µm
Width of cold arm, w_c	14	µm
Width of flexure, w_f	3	µm
Width of gripping arm	6	µm
Thickness of silicon substrate	20	µm
Thickness of silicon nitride	0.6	µm
Thickness of air gap	2	µm
Thickness of Poly1	2	µm
Thickness of Poly2	1.5	µm
Thickness of Metal	0.5	µm

IV. Numerical Model

The designed microgripper was simulated using finite element analysis (FEA) within the CoventorWare®

software. A three-dimensional (3D) model of the fabricated microgripper was developed (Fig. 4), and isotropic material properties were implemented to compute the electrothermomechanical solution (Table II). The actuating voltage was applied across the anchor pads of the actuator arm, while these same anchors were fixed in all directions. A homogeneous room temperature (300 K) was applied as an initial condition on all model elements, and the anchor pads were set to the constant substrate temperature, assumed to be equal to room temperature, throughout the analysis. The small dimensions of the actuator allowed the convective heat transfer coefficient of the bottom surface to be well approximated by conduction, through the stagnant 2 µm thick air layer and the silicon nitride layer, to the substrate. Convection from other surfaces as well as radiation can be reasonably ignored for thermal actuators operated at low operational power in still air [13]–[15].

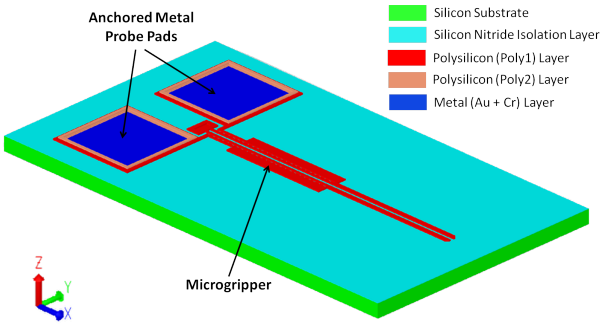

Fig. 4: A 3D model of the fabricated microgripper in CoventorWare®.

TABLE II: Material properties utilised for the microgripper simulation as obtained from the CoventorWare® Materials Library for the PolyMUMPs™ fabrication process. All properties are given at 300 K and all reference to polysilicon refer to the Poly1 structural layer.

Property	Value	Unit
Density of polysilicon	2.23	g/(cm)^3
Young's modulus of polysilicon, E	158	GPa
Poisson's ratio of polysilicon, ν	0.22	-
Thermal expansion coefficient of polysilicon, α	2.80	µm/mK
Specific heat capacity of polysilicon, c	100	J/kgK
Thermal conductivity of polysilicon, k_p	32	W/mK
Thermal conductivity of air, k_a	0.0262	W/mK
Thermal conductivity of silicon nitride, k_n	25	W/mK
Electrical resistivity of polysilicon	20	µΩm

V. Experimental Set-up

A set of dies with released microgripper structures were fabricated for experimental testing and characterisation. Electrical connections between the power supply and the contact pads of the microgripper were established using voltage probes, and two multimeters were used to measure the voltage and current applied to the structure. The displacement measurements of the microgripper arm tip were carried out using an optical microscope-based vision system with a camera embedded within the probe station (Fig. 5).

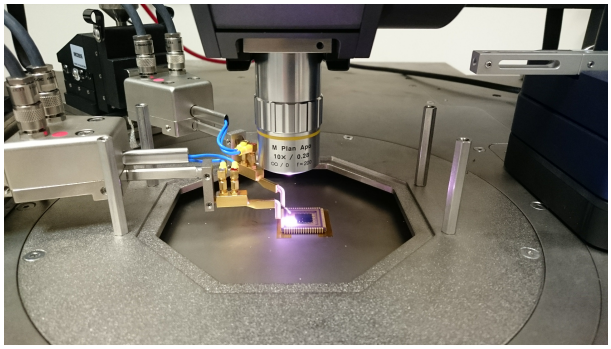

Fig. 5: The fabricated die enclosed in an integrated circuit package and mounted on the platform of the Cascade Microtech probe station with voltage probes to actuate the microgripper structure.

VI. Design and Fabrication Considerations

The experimental campaign enabled the identification of critical design and fabrication considerations essential to mitigate the malfunction or failure of the microgripper. These considerations are regarded as an important outcome of this work and are highlighted below.

A. Out-of-Plane Buckling

The lateral displacement obtained at the microgripper arm tips increases with an increase in the microgripper length for the same applied voltage. The microgripper length is however limited by the increased tendency of out-of-plane buckling of the thermal actuator's hot arm. Buckling will occur as a mode of failure on the hot arm if the developed compressive thermal load is greater than or equal to the critical buckling load (Fig. 6).

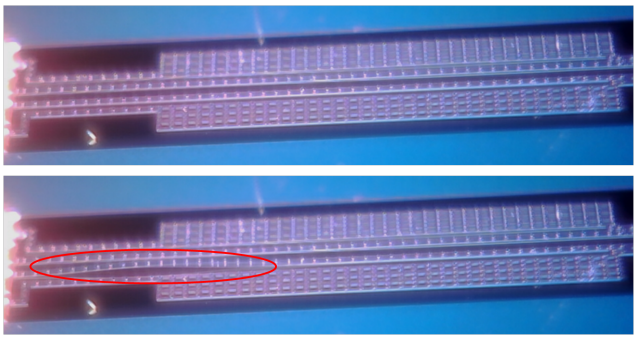

Fig. 6: Out-of-plane buckling of the microgripper's hot arm coming into effect (enclosed by red circle) when the compressive load within the hot arm exceeds the critical buckling load.

The compressive thermal load within the hot arm, F_c, is a result of the electrothermal actuation and is given by Eq. 1 [15]:

$$F_c = \frac{(2a^4 + 8a^3 - 12a^2 + 8a + 2)AEI\alpha\Delta T_{net}}{2(5a^4 I + a^4 {L_g}^2 A - 2a^3 I + 5aI + {L_g}^2 aA + I + a^5 I - 2a^2 I)} \quad (1)$$

where a is the ratio of the flexure length to the hot arm length, A is the cross-sectional area of the hot arm, E is the

Young's modulus of polysilicon, I is the moment of inertia of the hot arm about the axis of bending of buckling, α is the coefficient of thermal expansion of polysilicon, L_g is the length of the connector as shown in Fig. 2, and ΔT_{net} is the net temperature difference that takes into account the fact that as the hot arm expands, the cold arm and flexure components also slightly expand, thus reducing the net expansion difference between the hot and cold/flexure components. ΔT_{net} is thus defined as the temperature difference that would cause the same net expansion if applied to the hot arm alone, and is given by Eq. 2 [15]:

$$\Delta T_{net} = \frac{1}{L_h}\left[\int_0^{L_h} T_h dx - \int_0^{L_c} T_c dx - \int_0^{L_f} T_f dx\right] \quad (2)$$

where $T_h(x)$, $T_c(x)$ and $T_f(x)$ are the temperature distributions of the hot arm, cold arm and flexure components respectively, and can be obtained as detailed in [16]. L_c and L_f are the lengths of the cold arm and flexure components respectively as indicated in Fig. 2.

The critical buckling load in the hot arm, F_b, is defined as the load at which buckling occurs, and it is dependent on the hot arm geometry and material properties as given by Euler's formula in Eq. 3 [15]:

$$F_b = \frac{\pi^2 EI}{(KL_h)^2} \quad (3)$$

where E and I are as explained previously, and K is the beam effective length factor that is determined by the beam's end support conditions and that has a value of 0.5 for the hot arm considered here.

A microgripper should always be designed such that the thermal load within the hot arm is smaller than the best estimated critical buckling load. It can be observed from Eq. 3 that a wider and thicker hot arm (larger I), as well as a shorter hot arm (smaller L_h) will increase the critical buckling load, making the hot arm less susceptible to failure by buckling.

B. Fracture

Another important consideration is the investigation of the maximum stresses in terms of magnitude and location. In a normal microgripper design, the maximum stresses are usually located in the vicinity of the anchored probe pads. It must be ensured that these stresses are smaller that the ultimate tensile strength of the material in order to prevent fracture (Fig. 7). The use of round instead of sharp corners where the arms join the anchor pads is a design improvement that helps avoid the build-up of stress concentrations at these locations. Moreover, a sufficiently fine FEA mesh at the locations of the stress concentrations is essential as this has a very important effect on the resulting simulated stress values which are eventually used to assess whether the microgripper design is reliable or not. The frequency at which the ultrasonic wire bonding process is performed also needs to be considered to ensure that this frequency does not match the natural frequency of the structure, since it can lead to resonance of the arms and possible fracture close to the anchors.

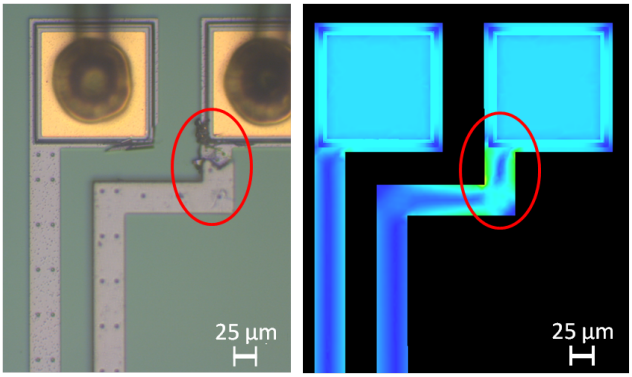

Fig. 7: Optical image (left) and numerical model (right) showing the damage caused on the microgripper arm due to the build-up of stresses larger than the ultimate tensile strength of the material.

C. Residual Stresses

In the PolyMUMPs™ fabrication process, the sacrificial PSG layers also act as the dopant source for the polysilicon. The final wafer is annealed at 1050^{o}C for 1 hour in a standard diffusion furnace during which the polysilicon is doped with phosphorus from the PSG layers above and below it. This process might introduce dopant concentration gradients across the beam cross-section, resulting in stress gradients and out-of-plane deformations in the polysilicon microgripper structure upon release (Fig. 8). This effect is dependent on the fabrication process parameters and may vary from one run to another.

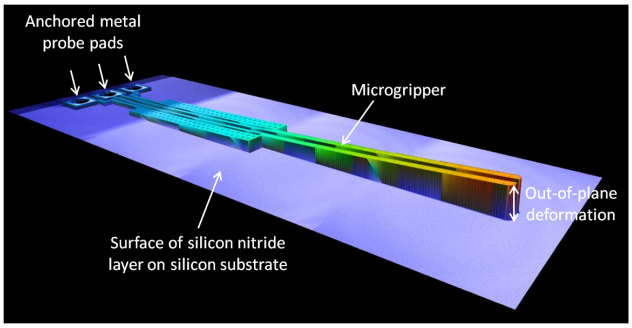

Fig. 8: Optical image of a microgripper structure using the Sensofar® 3D optical profilometer. The image shows the upward curling of the released structure at room temperature due to residual stresses incurred during device fabrication.

D. Stiction

A common problem encountered in surface micromachining fabrication processes such as PolyMUMPs™ is device stiction. This effect can be minimised by introducing dimples underneath the polysilicon beam as well as by subjecting the released dies to supercritical CO_2 drying following the HF solution release. Dimples are small bumps in the polysilicon layer (Fig. 3, Fig. 9) whose purpose is to reduce the contact

surface area and thus minimise device stiction to the substrate. The presence of silicon nitride as an electrical isolation layer between the polysilicon and the substrate is essential to prevent electrical shorting of the actuated structure in the case of dimples touching the substrate surface.

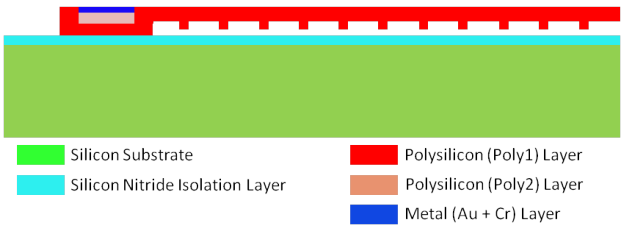

Fig. 9: Schematic cross-sectional view of the final PolyMUMPs™ microgripper structure (not-to-scale). The resulting air gap underneath the polysilicon beam is 2 µm while the thickness of the dimples is 0.75 µm.

VII. Experimental and Numerical Results

A. Thermal Analysis

In biomedical applications, the operating temperature of the microgripper plays a critical role due to the manipulation of living cells and biological tissues. The designed microgripper structure ensures that the maximum temperature is located near the middle of the hot arm while the cell gripping zone remains at room temperature even during actuation, making this device suitable for the safe handling of RBCs (Fig. 10).

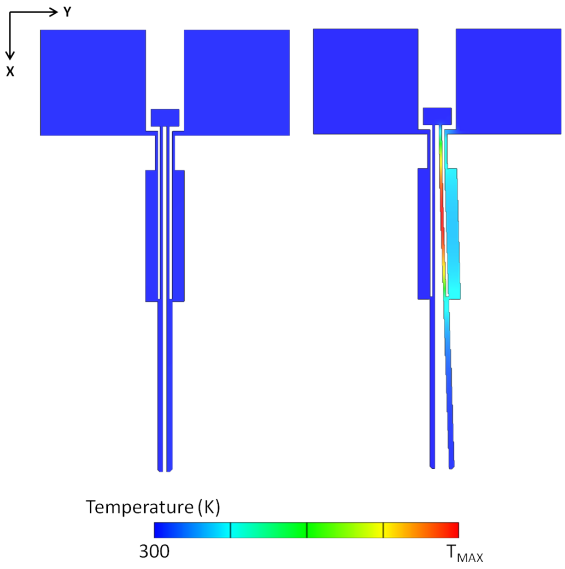

Fig. 10: Simulated steady-state temperature distribution of the microgripper: at no applied potential (left), and when one arm is subjected to an applied potential (right).

B. Structural Analysis

The displacement at the microgripper arm tips is generally one of the key factors optimised within the range of the microactuator functionality. This work deals with the design of a horizontal actuator, and thus the in-plane displacement (y-direction as shown in Fig. 11) is of the utmost interest. Fig. 11, Fig. 12 and Fig. 13 show the simulation and experimental measurement results of the displacement at the microgripper arm tip under an actuation voltage of 5 V. All comparisons show a good agreement between the results of the numerical and experimental work. The current and power dissipated across the actuated microgripper arm as a function of the applied voltage are given in Fig. 14.

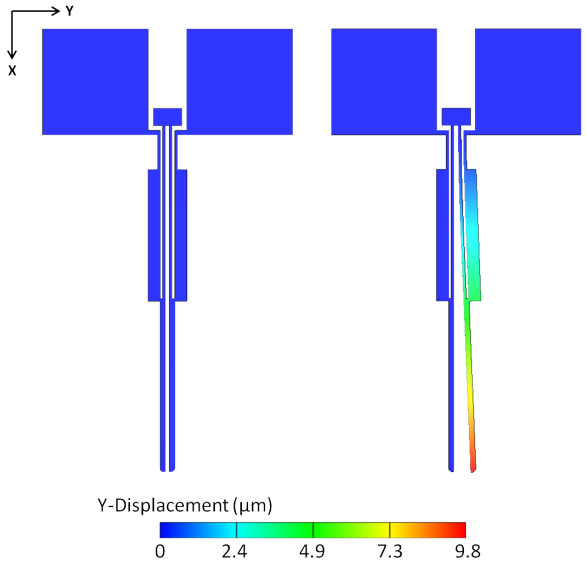

Fig. 11: Simulation results showing the designed polysilicon microgripper structure when not actuated (left), and with one arm undergoing a y-displacement of 9.8 µm under an applied potential of 5 V (right).

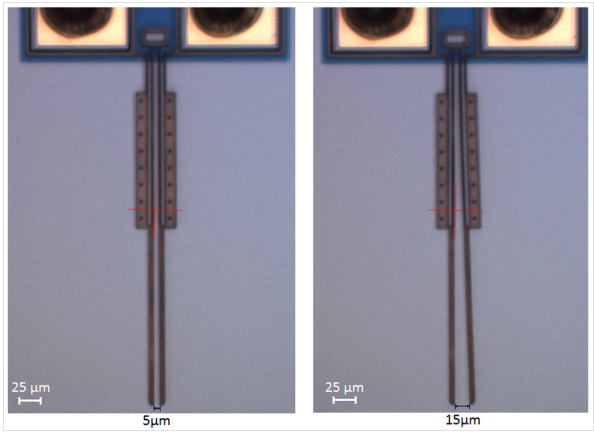

Fig. 12: Optical images showing the fabricated microgripper when not actuated (left), and with one arm actuated under an applied potential of 5 V (right). The initial opening between the microgripper arms (zero actuation voltage) was 5 µm. The microgripper arm was tested under an applied potential of 5 V and the gap increased to 15 µm, resulting in an arm movement of 10 µm.

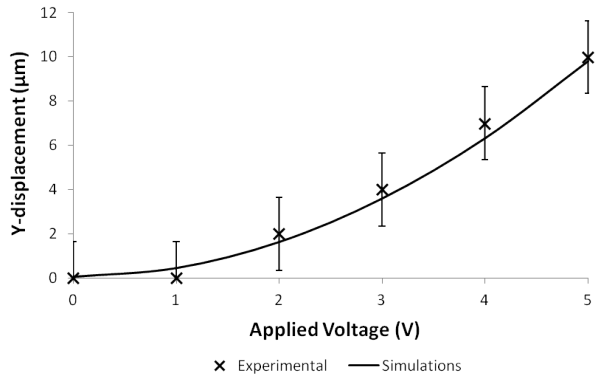

Fig. 13: Comparison of the numerical and experimental results for the microgripper arm tip displacement as a function of applied voltage.

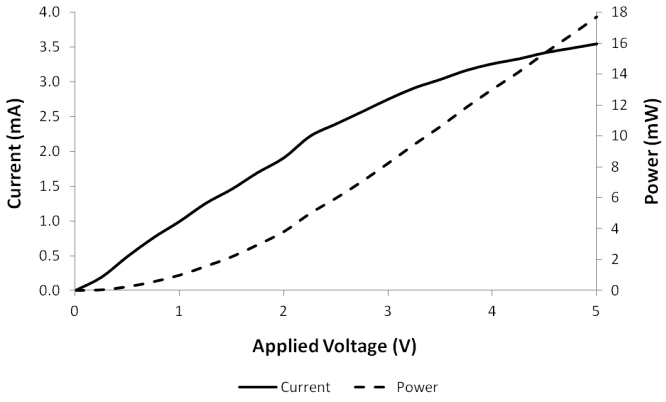

Fig. 14: Variations of current, and power dissipated, with voltage across one microgripper arm.

VIII. Conclusions

This paper has presented the design, numerical modelling, fabrication, and experimental testing of a horizontal electrothermal MEMS microgripper suitable for the deformability characterisation of RBCs. The 'hot and cold arm' polysilicon microgripper was designed by considering the PolyMUMPs™ fabrication constraints in terms of dimensions, aspect ratio and material properties. An FEA model of the microgripper was developed in CoventorWare® and electrothermomechanical simulations were carried out, taking into account the internal heat generation due to the applied potential, as well as conduction heat losses to both the substrate and the anchor pads.

The fabricated microgripper was successfully tested, and the measured displacements of the actuated microgripper arm tip are presented with respect to the applied voltage. Numerical results for the microgripper's opening displacements are also presented and compared with the experimental results, and good agreement is observed. Critical microgripper design and fabrication considerations were derived from this work, with each consideration in need of further detailed investigations. These considerations have been proposed to mitigate microgripper malfunction or failure mechanisms related to out-of-plane buckling of the hot arm, fracture of the arms in the vicinity of the anchored contact pads, device stiction as well as out-of-plane deformations resulting from residual stresses incurred during the device fabrication.

Acknowledgments

The research work disclosed in this publication is funded by the Reach High Scholars Programme - Post-Doctoral Grants. The grant is part-financed by the European Union, Operational Programme II - Cohesion Policy 2014-2020 Investing in human capital to create more opportunities and promote the wellbeing of society - European Social Fund.

References

[1] R. Zhang, J. Chu, H. Wang, Z. Chen, "A multipurpose electrothermal microgripper for biological micro-manipulation," Microsyst. Tech., vol. 19, no. 1, pp. 89-97, 2013.

[2] K. Ivanova et al., "Thermally driven microgripper as a tool for micro assembly," Microelectronic Engineering, vol. 83, no. 4-9, pp. 1393-1395, 2006.

[3] Y. Jia, Q. Xu, "MEMS microgripper actuators and sensors: the state-of-the-art survey," Recent Patents on Mechanical Engineering, vol. 6, no. 2, pp. 132-142, 2013.

[4] S. Yang, Q. Xu, "A review on actuation and sensing techniques for MEMS-based microgrippers," Journal of Micro-Bio Robotics, vol. 13, no. 1-4, pp. 1-14, 2017.

[5] N. Chronis, L.P. Lee, "Electrothermally activated SU-8 microgripper for single cell manipulation in solution", Journal of Microelectromechanical Systems, vol. 14, no. 4, pp. 857-863, 2005.

[6] P. Di Giamberardino, A. Bagolini, P. Bellutti, I.J. Rudas, M. Verotti, F. Botta, N.P. Belfiore, "New MEMS tweezers for the viscoelastic characterization of soft materials at the microscale," Micromachines, vol. 9, no. 1, article no. 15, 2017.

[7] K. Kim, X. Liu, Y. Zhang, J. Cheng, W.X. Yu, Y. Sun, "Elastic and viscoelastic characterization of microcapsules for drug delivery using a force-feedback MEMS microgripper," Biomed Microdevices, vol. 11, no. 2, pp. 421-427, 2009.

[8] B.N. Zaitsev, "Blood Cells Study," NT-MDT Spectrum Instruments, State Research Center of Virology and Biotechnology VECTOR, Koltsovo, Novosibirsk Oblast, Russia, 2015.

[9] G. Tomaiuolo, "Biomechanical properties of red blood cells in health and disease towards microfluidics," Biomicrofluidics, vol. 8, no. 5, pp. 051501, 2014.

[10] B. Hannon and M. Ruth, "Malaria and sickle cell anemia," In: "Dynamic modeling of diseases and pests," Springer New York, New York, pp. 63-81, 2009.

[11] M. Cauchi, P. Mollicone, I. Grech, B. Mallia, N. Sammut, "Design and analysis of a MEMS-based electrothermal microgripper," In: "Proceedings of International CAE Conference 2016," Parma, Italy, October 2016.

[12] A. Cowen, B. Hardy, R. Mahadevan and S. Wilcenski, "Polymumps design handbook," MEMSCAP Inc., Rev. 13.0, 2011.

[13] Qing An Huang and Neville Ka Shek Lee, "Analysis and design of polysilicon thermal flexure actuator," Journal of Micromechanics and Microengineering, vol. 9, no. 1, pp. 64-70, 1999.

[14] R. A. Coutu, R. S. LaFleur, J. P. K. Walton and L. A. Starman, "Thermal management using MEMS bimorph cantilever beams," Experimental Mechanics, vol. 56, no. 7, pp. 1293-1303, 2016.

[15] R. Hickey, M. Kujath and T. Hubbard, "Heat transfer analysis and optimization of two-beam microelectromechanical thermal actuators," Journal of Vacuum Science & Technology A: Vacuum, Surfaces, and Films, vol. 20, no. 3, pp. 971-974, 2002.

[16] M. Cauchi, I. Grech, B. Mallia, P. Mollicone and N. Sammut, "Analytical, Numerical and Experimental Study of a Horizontal Electrothermal MEMS Microgripper for the Deformability Characterisation of Human Red Blood Cells," Micromachines, vol. 9, no. 3, article no. 108, 2018.